Supporting Information

Synthesis and characterization of high grafting density bottle-brush poly(oxa)norbornene-*g*-poly(ε-caprolactone)

Duc Anh N'Guyen, Flavien Leroux, Véronique Montembault, Sagrario Pascual and Laurent Fontaine[*]

Institut des Molécules et Matériaux du Mans (IMMM), Equipe Méthodologie et Synthèse des Polymères, UMR CNRS 6283, Université du Maine, Avenue Olivier Messiaen, 72085 Le Mans Cedex 9, France

* Corresponding author: laurent.fontaine@univ-lemans.fr

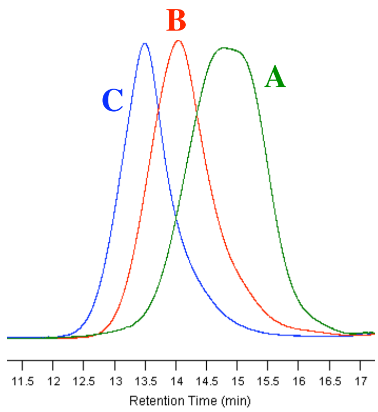

Figure S1. SEC traces for the (A) **OX-PCL$_{24}$** (Table 1, run 1), (B) **OX-PCL$_{52}$** (Table 1, run 2) and (C) **OX-PCL$_{92}$** (Table 1, run 3).

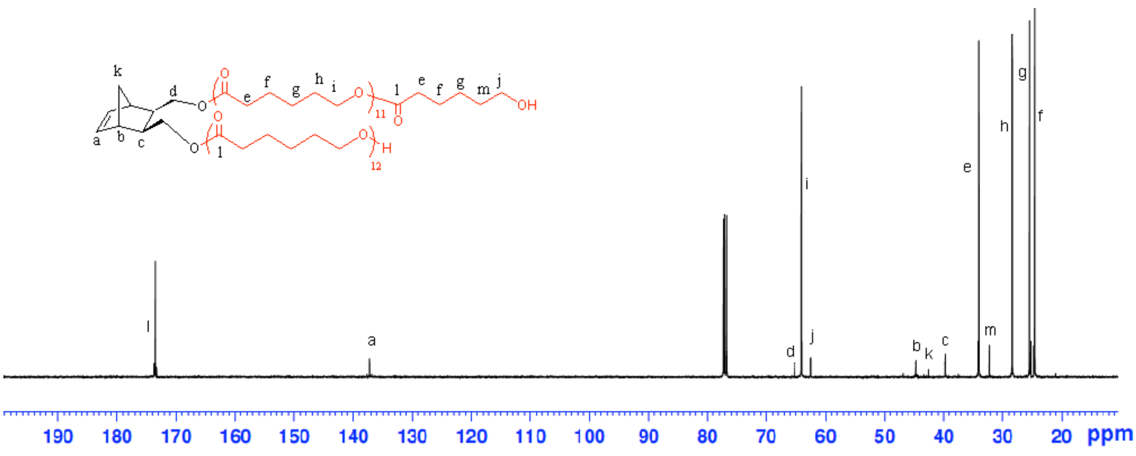

Figure S2. ^{13}C NMR spectrum (100 MHz, $CDCl_3$, 25 °C) of precipitated **NB-PCL$_{24}$** from the ROP of CL in THF at 25°C using **NB** as the initiator and TBD as the catalyst with $[CL]_0/[\mathbf{NB}]_0 = 20$ (Table 1, run 4).

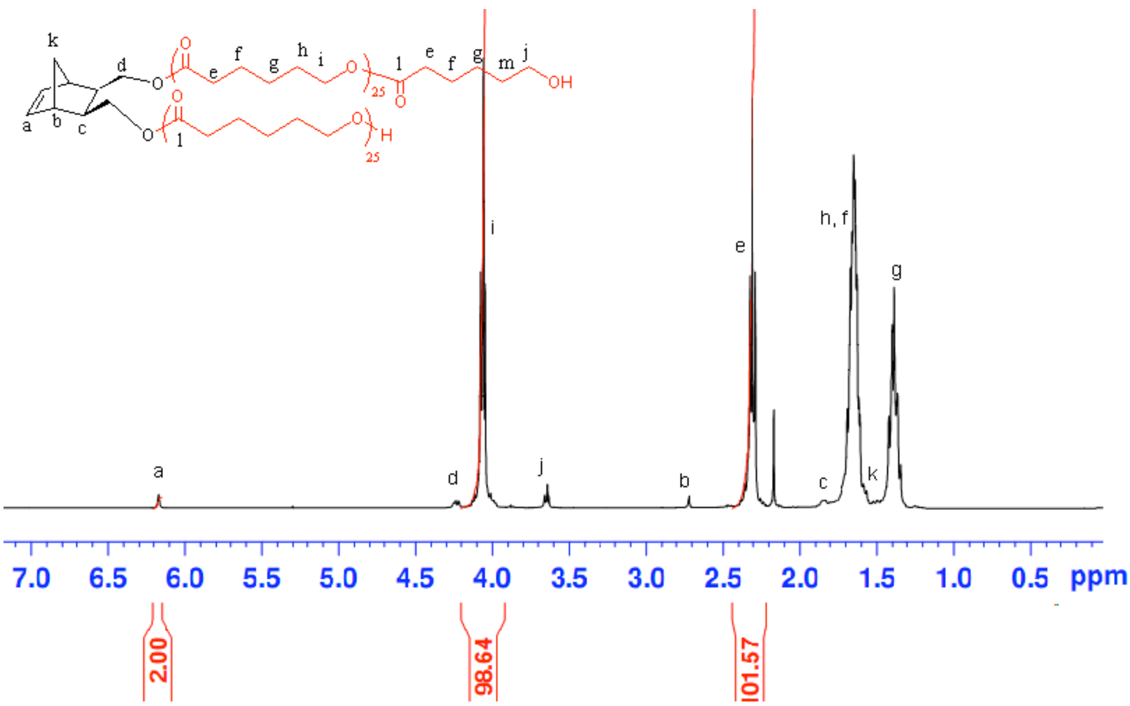

Figure S3. ^{1}H NMR spectrum (400 MHz, $CDCl_3$, 25 °C) of precipitated **NB-PCL$_{51}$** from the ROP of CL in THF at 25°C using **NB** as the initiator and TBD as the catalyst with $[CL]_0/[\mathbf{NB}]_0 = 48$ (Table 1, run 5).

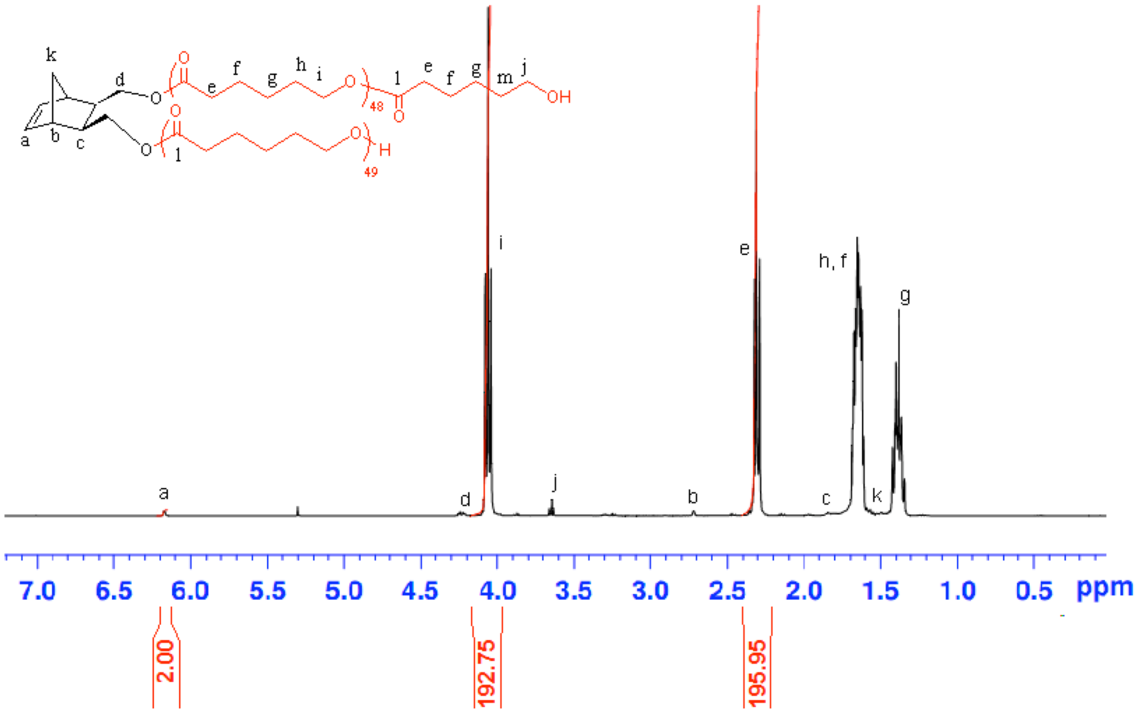

Figure S4. ^{1}H NMR spectrum (400 MHz, $CDCl_3$, 25 °C) of precipitated **NB-PCL$_{98}$** from the ROP of CL in THF at 25°C using **NB** as the initiator and TBD as the catalyst with $[CL]_0/[\mathbf{NB}]_0 = 96$ (Table 1, run 6).

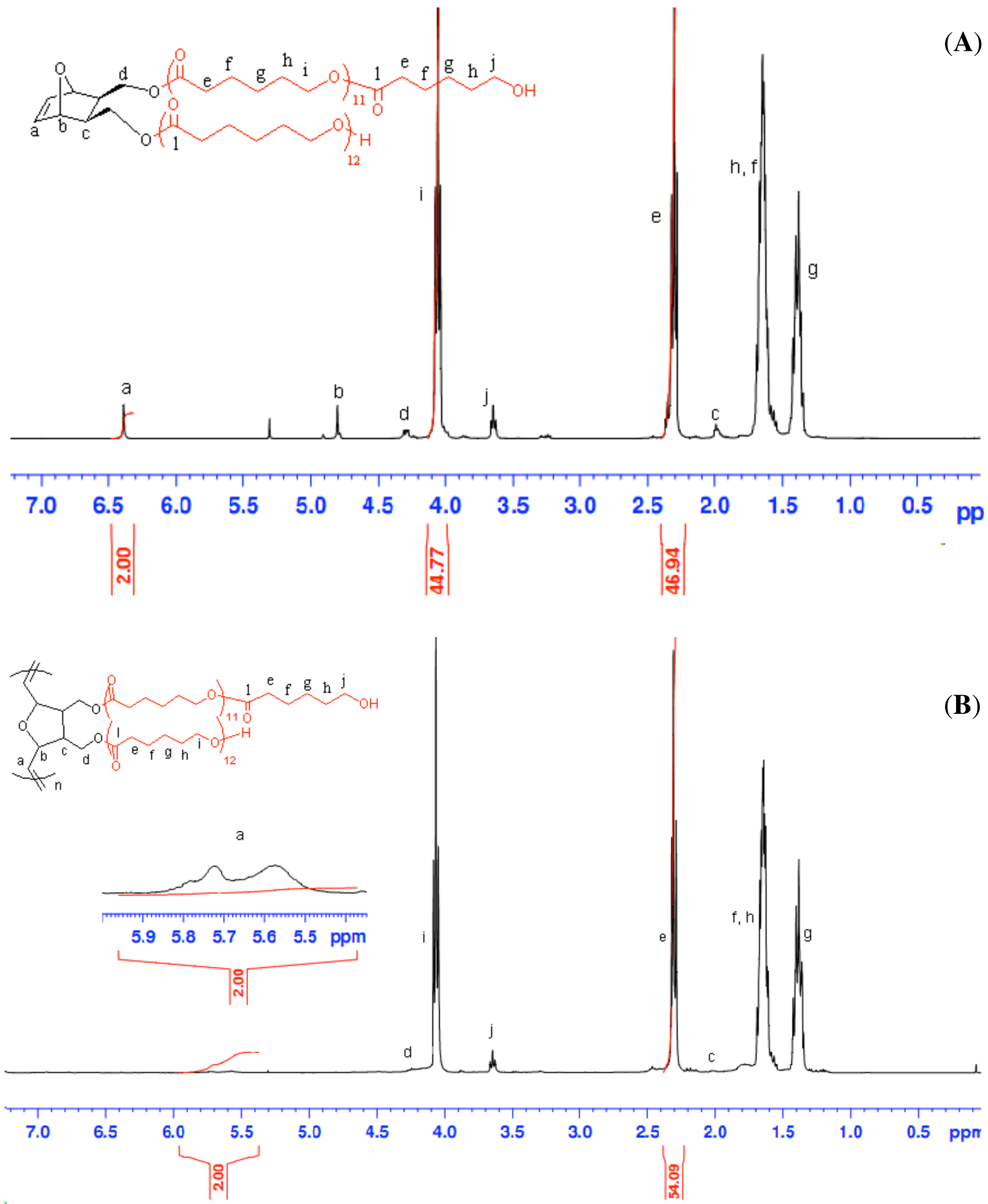

Figure S5. [1]H NMR spectra (400 MHz, $CDCl_3$, 25 °C) of (A) precipitated **OX-PCL$_{24}$** from the ROP of CL in THF at 25°C using **OX** as the initiator and TBD as the catalyst with $[CL]_0/[\mathbf{OX}]_0 = 20$ (Table 1, run 1) and (B) crude **POX$_{10}$-*g*-PCL$_{24}$** obtained from the ROMP of **OX-PCL$_{24}$** in toluene at 70°C using **G2** as the catalyst with [**OX-PCL$_{24}$**]/[**G2**] = 10 for a reaction time of 3 h (Table 2, run 1).

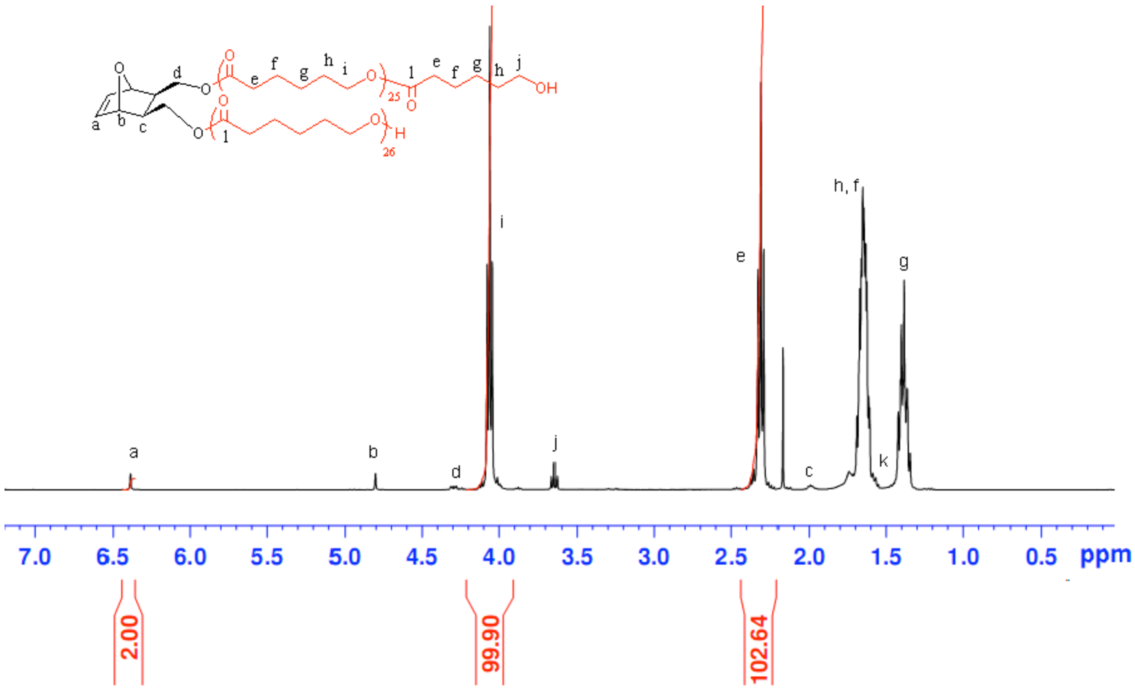

Figure S6. ^{1}H NMR spectrum (400 MHz, $CDCl_3$, 25 °C) of precipitated **OX-PCL$_{52}$** from the ROP of CL in THF at 25°C using **OX** as the initiator and TBD as the catalyst with $[CL]_0/[\mathbf{OX}]_0 = 48$ (Table 1, run 2).

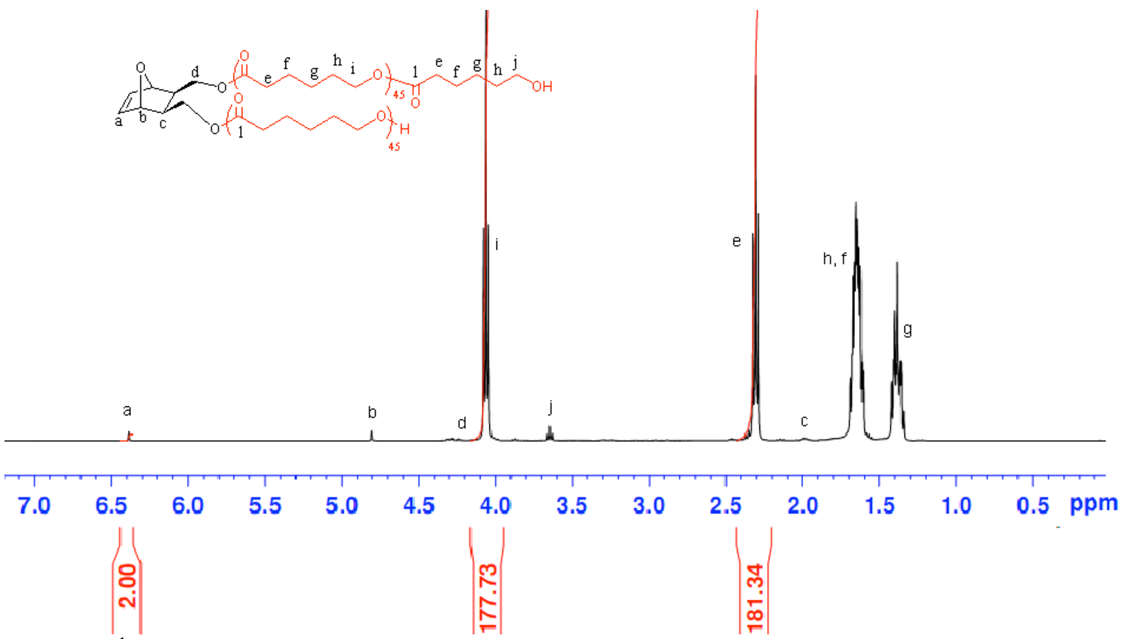

Figure S7. ^{1}H NMR spectrum (400 MHz, $CDCl_3$, 25 °C) of precipitated **OX-PCL$_{92}$** from the ROP of CL in THF at 25°C using **OX** as the initiator and TBD as the catalyst with $[CL]_0/[\mathbf{OX}]_0 = 96$ (Table 1, run 3).

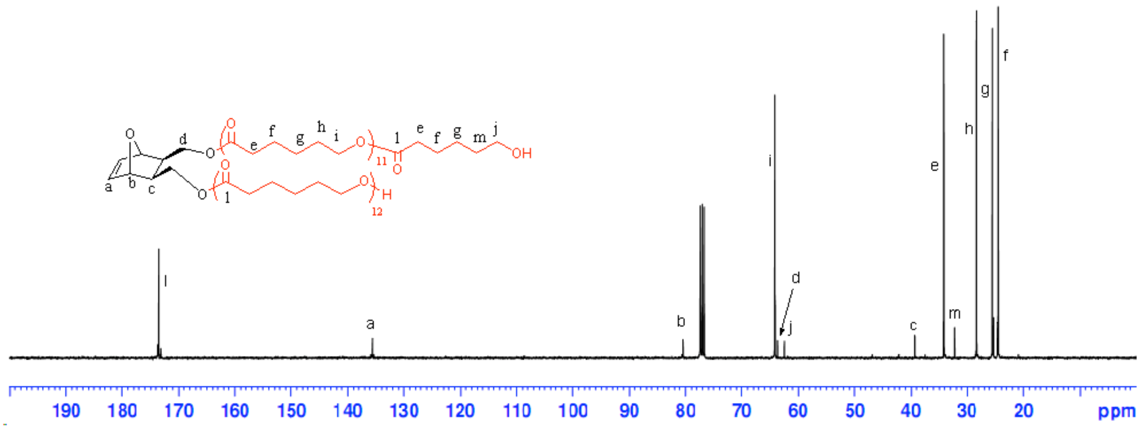

Figure S8. ^{13}C NMR spectrum (100 MHz, $CDCl_3$, 25 °C) of precipitated **OX-PCL$_{24}$** from the ROP of CL in THF at 25°C using **OX** as the initiator and TBD as the catalyst with $[CL]_0/[\mathbf{OX}]_0 = 20$ (Table 1, run 1).

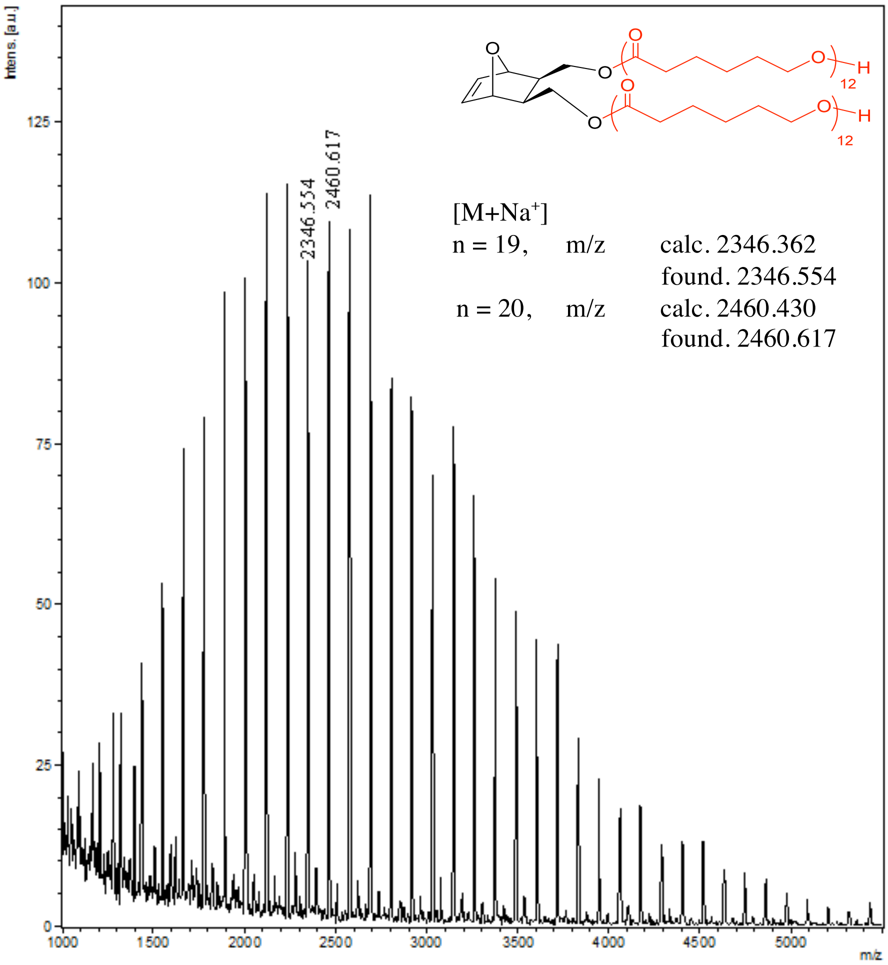

Figure S9. MALDI-TOF mass spectrum (matrix: *trans*-2-[3-(4-*tert*-butylphenyl)-2-methyl-2-propenylidene]malononitrile (DCTB) + sodium trifluoroacetate (NaTFA)) of the PCL-based norbornene synthesized by ROP using **OX** as the initiator and TBD as the catalyst in THF at 25°C with $[CL]_0/[\mathbf{OX}]_0$ = 20/1 (Table 1, run 1).

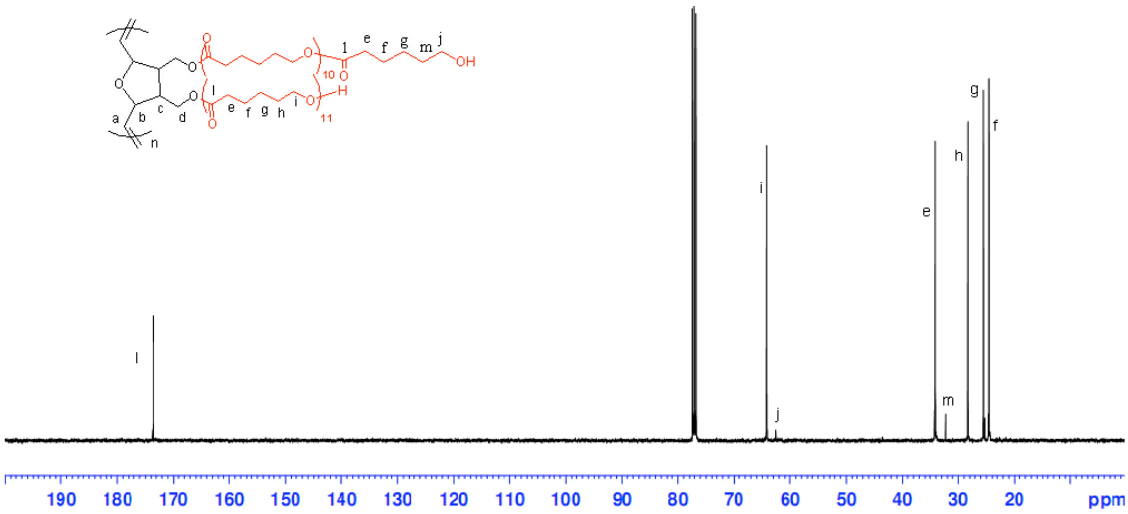

Figure S10. [13]C NMR spectrum (100 MHz, $CDCl_3$, 25 °C) of **POX$_{10}$-*g*-PCL$_{24}$** obtained from the ROMP of **OX-PCL$_{24}$** in toluene at 70°C using **G2** as the catalyst with [**OX-PCL$_{24}$**]/[**G2**] = 10 for a reaction time of 3 h (Table 2, run 1).

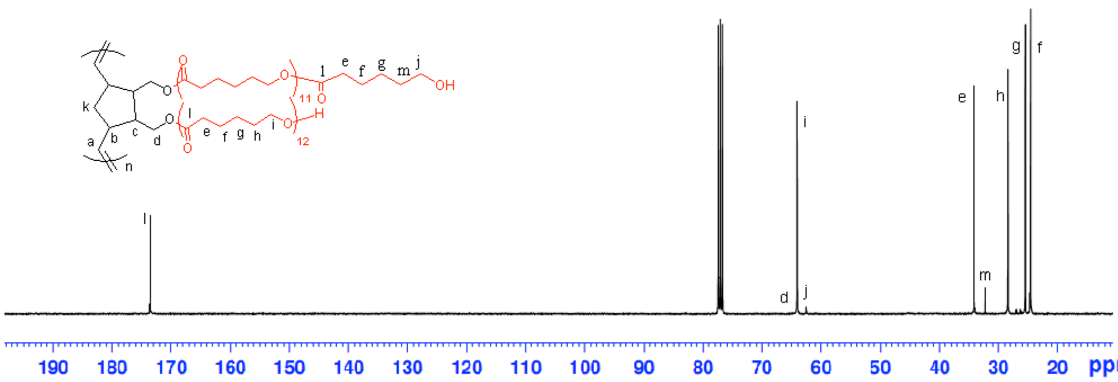

Figure S11. [13]C NMR spectrum (100 MHz, $CDCl_3$, 25 °C) of **PNB$_{10}$-*g*-PCL$_{24}$** obtained from the ROMP of **NB-PCL$_{24}$** in toluene at 70°C using **G2** as the catalyst with [**NB-PCL$_{24}$**]/[**G2**] = 10 for a reaction time of 3 h (Table 2, run 8).

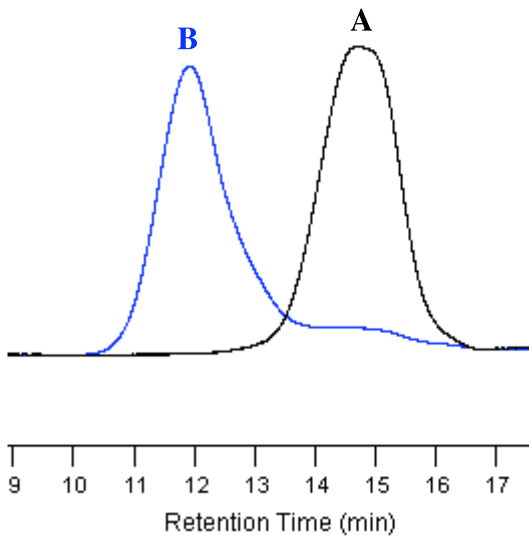

Figure S12. SEC traces for the (A) precipitated **OX-PCL$_{24}$** (Table 1, run 1) and (B) crude **POX$_{10}$-*g*-PCL$_{24}$** obtained by ROMP of **OX-PCL$_{24}$** initiated by **G2** (Table 2, run 1).

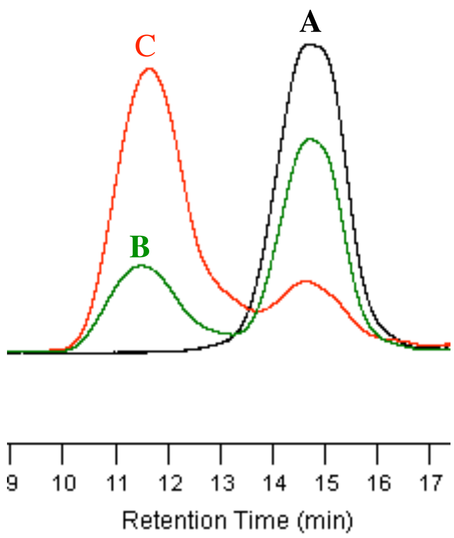

Figure S13. SEC traces for the (A) precipitated **OX-PCL$_{24}$** (Table 1, run 1), (B) crude **POX$_{50}$-*g*-PCL$_{24}$** (Table 2, run 2) and (C) crude **POX$_{100}$-*g*-PCL$_{24}$** (Table 2, run 3) obtained by ROMP of **OX-PCL$_{24}$** initiated by **G2**.

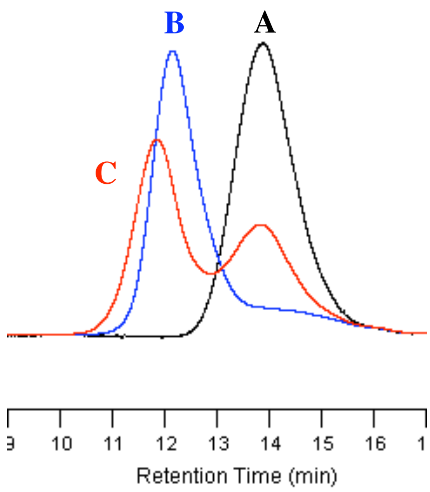

Figure S14. SEC traces for the (A) precipitated **OX-PCL$_{52}$** (Table 1, run 2), (B) crude **POX$_{10}$-*g*-PCL$_{52}$** (Table 2, run 4) and (C) crude **POX$_{50}$-*g*-PCL$_{52}$** (Table 2, run 5) obtained by ROMP of **OX-PCL$_{52}$** initiated by **G2**.

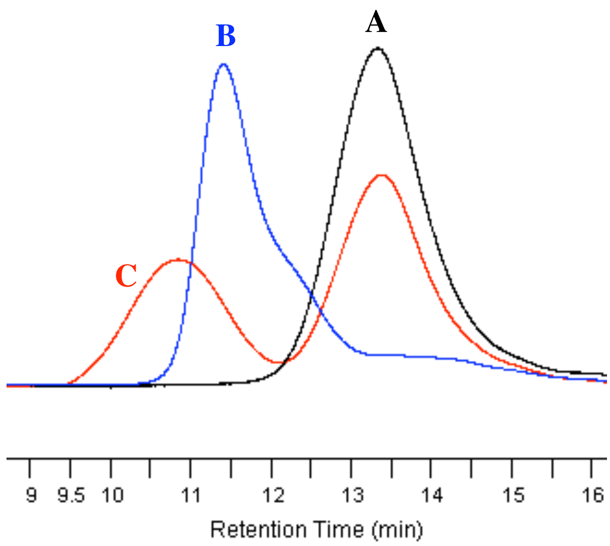

Figure S15. SEC traces for the (A) precipitated **OX-PCL$_{92}$** (Table 1, run 3), (B) crude **POX$_{10}$-*g*-PCL$_{92}$** (Table 2, run 6) and (C) crude **POX$_{50}$-*g*-PCL$_{92}$** (Table 2, run 7) obtained by ROMP of **OX-PCL$_{92}$** initiated by **G2**.

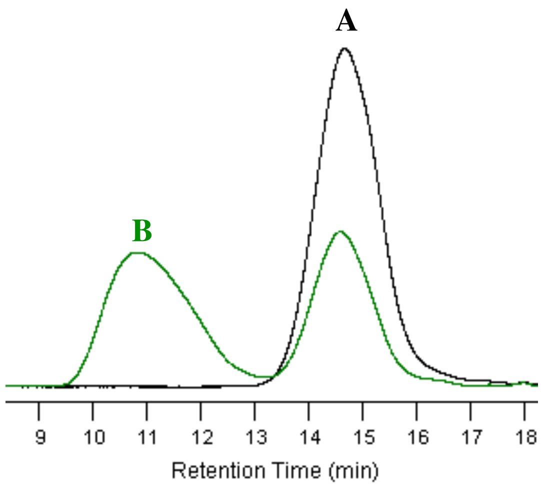

Figure S16. SEC traces for the (A) precipitated **NB-PCL$_{24}$** (Table 1, run 4) and (B) crude **PNB$_{100}$-*g*-PCL$_{24}$** obtained by ROMP of **NB-PCL$_{24}$** initiated by **G2** (Table 2, run 10).

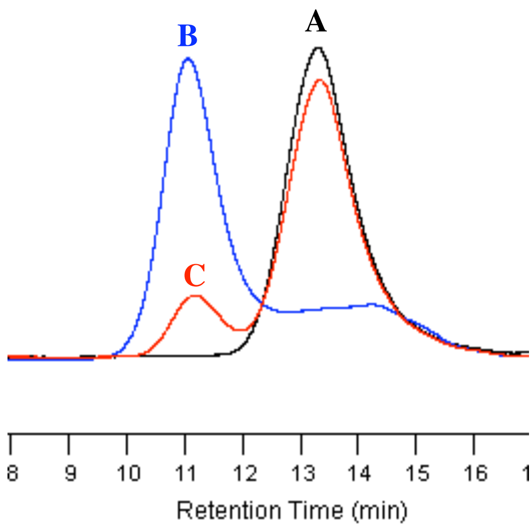

Figure S17. SEC traces for the (A) precipitated **NB-PCL$_{98}$** (Table 1, run 6), (B) crude **PNB$_{10}$-*g*-PCL$_{98}$** (Table 2, run 16) and (C) crude **PNB$_{50}$-*g*-PCL$_{98}$** (Table 2, run 17) obtained by ROMP of **NB-PCL$_{98}$** initiated by **G2**.

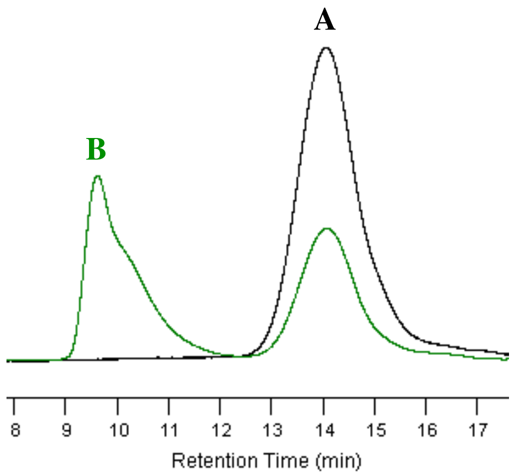

Figure S18. SEC traces for the (A) precipitated **NB-PCL$_{51}$** (Table 1, run 4) and (B) crude **PNB$_{200}$-*g*-PCL$_{51}$** (Table 2, run 15) obtained by ROMP of **NB-PCL$_{51}$** initiated by **G3'**.

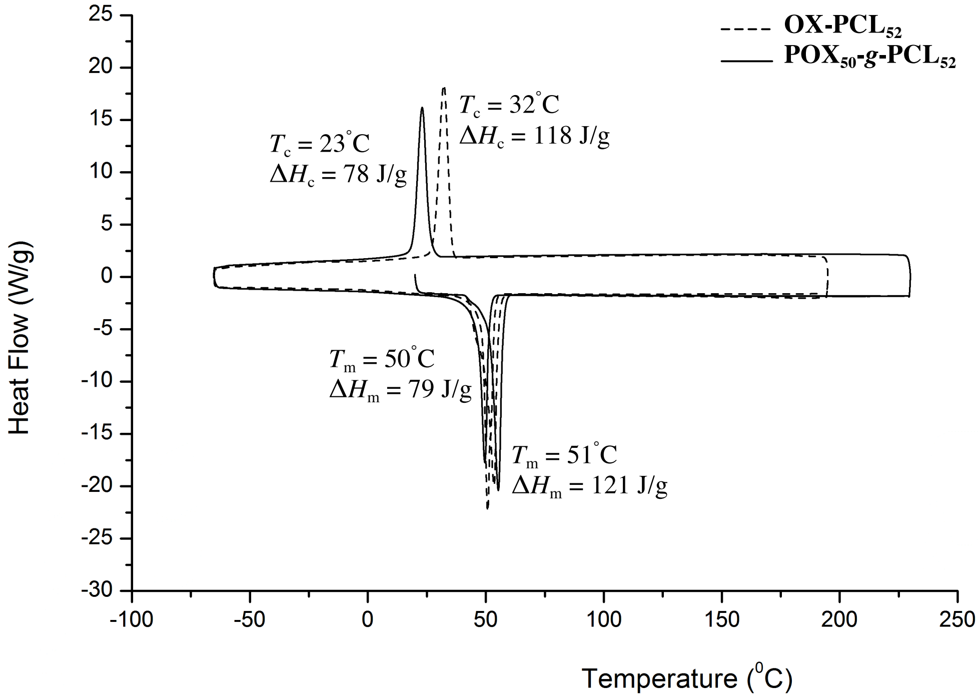

Figure S19. DSC traces of **POX$_{50}$-*g*-PCL$_{52}$** (full line) (Table 2, run 5) and **OX-PCL$_{52}$** (dashed line) (Table 1, run 2).

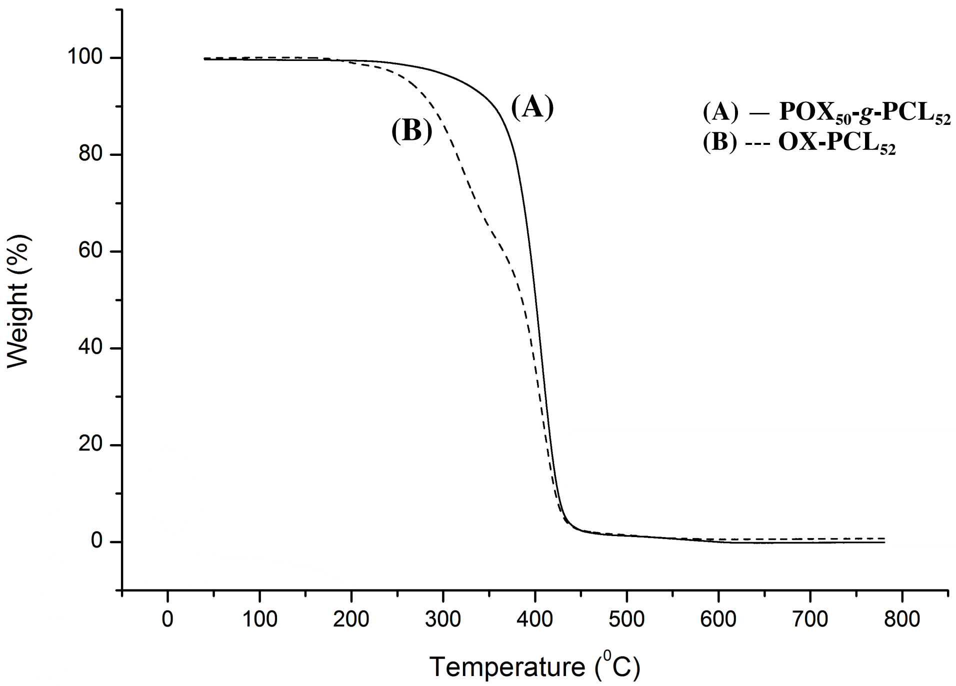

Figure S20. Comparison of TGA curves for (A) **POX$_{50}$-*g*-PCL$_{52}$** (full line) (Table 2, run 5) and (B) **OX-PCL$_{52}$** (dashed line) (Table 1, run 2).